Review Book: "Recent Research Developments in Optics"

Title: **Optical Methods for Interdisciplinary Research in the Coastal Ocean**

Authors: Grace Chang, Tommy Dickey, Songnian Jiang, Derek Manov, and Frank Spada

Affiliation: Ocean Physics Laboratory, University of California at Santa Barbara,
6487 Calle Real Suite A, Goleta, CA 93117, U.S.A.; e-mail: grace.chang@opl.ucsb.edu

Running Title: Coastal Ocean Optical Oceanography

ABSTRACT

Ocean optics provides a valuable tool for understanding physical, biological, chemical, and geological processes in the coastal ocean. Studies of coastal ocean ecology including health of the ocean (e.g., harmful algal blooms and pollutant dispersal), the carbon budget, parameters affecting and affected by the heat budget, and global warming are greatly facilitated with ocean optics. Optical data provide essential information about particulate concentration, type, and size distribution, primary production, and water column turbidity. In addition, optical data can be correlated with complementary physical, biological, chemical, and geological data to identify and track water mass movements in the coastal ocean. Most importantly, optical research methods can be performed with commercially available instrumentation and relatively simple algorithms and models. The present review is intended to provide (1) a brief synopsis of concepts in ocean optics including definitions of optical terms, (2) a summary of recent advances in ocean optical instrumentation and research platforms used in the coastal ocean, and (3) an introduction to optical data analysis methods used in coastal ocean research.

INTRODUCTION

Ocean optics concerns the study of light and its propagation through the oceanic water column and reflection off of the ocean surface. Bio-optics is the study of biological effects on optical properties and *vice versa*. The terms ocean optics, marine optics, hydrologic optics, and bio-optics are related and often used interchangeably. Previous studies of optics involved theoretical aspects of the physics of light through a water body (e.g. : [1,2,3]). Over the past several decades, this theoretical research has led to many advances in oceanic optical technology and in turn, new measurements have been vital for developing novel theories and models ([4,5]). Recently, optical and bio-optical research has emphasized the use of optics as a tool for understanding physical, chemical, biological, and geological oceanography. Biogeochemistry is a new research area that complements much of the research of bio-optical oceanography.

Fundamentally, phytoplankton depend on light and light utilization. Therefore, knowledge of optics and bio-optics is essential for the understanding of primary productivity (on physiological and oceanographic scales), ocean ecology, and the carbon cycle. The penetration of solar radiation is affected by the optical properties of the upper water column. Light penetration, and thus the thermal structure and heat budget, are altered by the absorption and scattering by the water itself as well as particulates and dissolved matter in the upper ocean. Variability of the heat budget as well as sources and sinks of carbon in the ocean affect and are affected by global climate change, which has great implications on Earth's ecology. Environmental concerns can also be addressed using ocean optics. Variability in turbidity (or water clarity) is an indicator of changes in concentrations, size distributions, or types of water column constituents (e.g., sediments; phytoplankton, including harmful algae; dissolved organic matter; and pollutants). Underwater visibility is also important to military and industrial activity. Current optical research is focusing on the use of optical properties as tracers to better comprehend water mass movements, e.g., river and estuarine flows, fronts, jets, and eddies. Also, the advent of ocean color remote sensing technology based on optics is allowing scientists to investigate oceanographic processes and characteristics synoptically.

The present review is intended to provide (1) a brief synopsis of concepts in ocean optics including definitions of optical terms, (2) a summary of recent advances in ocean optical instrumentation and research platforms used in the coastal ocean, and (3) an introduction to optical data analysis methods used in coastal ocean research.

CONCEPTS IN OCEAN OPTICS

A brief review of the fundamentals of ocean optics is presented below. Detailed definitions, mathematical formulations, and diagrams can be found in books by Kirk ([2]) and Mobley ([3]) and in International Ocean Colour Coordinating Group Reports, Numbers 2 and 3 ([6,7]).

Apparent optical properties

Apparent optical properties (AOPs) are properties that depend on the constituents of the aquatic medium (pure seawater, phytoplankton, detritus, and gelbstoff), the geometry of the subsurface light field, and the wavelength of the electromagnetic radiation. The most commonly and easily measured AOPs are radiance and irradiance. Radiance, $L(\theta,\Phi,\lambda)$, is the radiant light flux at a specified point in a given direction per unit solid angle, per unit area perpendicular to the direction of light propagation, at a specific wavelength (units of W (or quanta s^{-1}) m^{-2} sr^{-1}) (Figure 1.3 in Kirk, [2]). Zenith angle, θ, is the angle between a vertical line perpendicular to a flat plate and an incident light beam, and azimuthal angle, Φ, is the angle with respect to a reference line in the plane of the flat plate. Wavelength, λ, is generally measured in the visible, between 400 and 700 nm. Important radiance quantities include the upwelling radiance, $L_u(\lambda)$, and the water-leaving radiance, $L_w(\lambda)$. Upwelling radiance is the radiant light flux in the upward direction and $L_w(\lambda)$ is $L_u(\lambda)$ extrapolated just through the ocean surface.

Irradiance is the radiant flux per unit surface area (units of W m^{-2} nm^{-1} or quanta (or photons) m^{-2} s^{-1} or mol quanta (or photons) m^{-2} s^{-1}). Downwelling irradiance, $E_d(\lambda)$, is the irradiance of a downwelling light stream impinging on the top face of a horizontal plane and upwelling irradiance, $E_u(\lambda)$, is the irradiance of an upwelling light stream impinging on the bottom face of a horizontal plane. Net downward irradiance, $E_n(\lambda)$, is the difference between downwelling and upwelling irradiance, $E_n(\lambda) = E_d(\lambda) - E_u(\lambda)$, or the integral of $L(\theta,\Phi,\lambda) \cos\theta$ over all angles (full solid angle 4π). Scalar irradiance, $E_0(\lambda)$, is defined as the integral of $L(\theta,\Phi,\lambda)$ over all angles. The biologically important quantity called photosynthetically available radiation, or PAR, is obtained by integrating scalar irradiance over the visible wavelengths (400 to 700 nm).

AOP relationships of interest are the average cosine for total light, $\mu(\lambda) = E_n(\lambda)/E_0(\lambda)$, the irradiance reflectance (or irradiance ratio), $R(\lambda) = E_u(\lambda)/E_d(\lambda)$, and the spectral radiance reflectance, $r_{rs}(\lambda) = L_u(\lambda)/E_d(\lambda)$ (sr^{-1}). The important quantity that is measured by remote sensors, remote sensing reflectance, $R_{rs}(\lambda)$, is simply $r_{rs}(\lambda)$ taken just above the sea surface, $R_{rs}(\lambda) = L_w(\lambda)/E_d(\lambda)$. Radiance and irradiance measurements are fundamentally important for quantifying the amount of light available for photosynthesis, heating of the upper ocean, radiative transfer theory, and the interpretation and quantification of remotely sensed data.

Inherent optical properties (IOPs)

Properties that are dependent only upon the medium itself (independent of the ambient light field and its geometrical distribution) are termed inherent optical properties (IOPs). IOPs are based on the principle that photons in an aquatic medium can only be absorbed or scattered. The absorption and scattering properties are quantified in terms of the IOPs: absorption coefficient, $a(\lambda)$, scattering coefficient, $b(\lambda)$, beam attenuation coefficient, $c(\lambda) = a(\lambda) + b(\lambda)$ (also called beam c), and volume scattering function, $\beta(\psi, \lambda)$, where ψ is the scattering angle and λ is light wavelength. The IOPs $a(\lambda)$, $b(\lambda)$, and $c(\lambda)$ all have units of m^{-1}. $\beta(\psi, \lambda)$ represents the scattered intensity of light per unit incident irradiance per unit volume of water at some angle ψ into solid angle element $\Delta\Omega$, with units of m^{-1} sr^{-1}. The scattering coefficient, $b(\lambda)$, is obtained by difference $b(\lambda) = c(\lambda) - a(\lambda)$ or by integrating $\beta(\psi, \lambda)$ over all solid angles. The forward scattering coefficient, $b_f(\lambda)$, is obtained by integrating over $\psi = 0$ to $\pi/2$ and the backward scattering coefficient, $b_b(\lambda)$, is calculated by integrating over the backward-looking hemisphere ($\psi = \pi/2$ to π). The volume scattering phase function, $\beta_p(\psi, \lambda)$, normalizes the volume scattering function by the total scattering, $= \beta(\psi, \lambda)/b(\lambda)$ (sr^{-1}). The single-scattering albedo, $\omega_0(\lambda) = b(\lambda)/c(\lambda)$, characterizes the proportion of light which is scattered versus that which is absorbed. The single-scattering assumption fails when there are high concentrations of strongly scattering particles and when there are long pathlengths of light (e.g., sunrise and sunset).

Total absorption, scattering, and attenuation coefficients can be partitioned into the four constituents of the aquatic medium in natural oceanic waters: pure seawater (w), phytoplankton (ph), detritus (d), and gelbstoff (g) (e.g. : [8,9,10]): $a_t(\lambda) = a_w(\lambda) + a_{ph}(\lambda) + a_d(\lambda) + a_g(\lambda)$, $b_t(\lambda) = b_w(\lambda) + b_{ph}(\lambda) + b_d(\lambda)$, and $c_t(\lambda) = c_w(\lambda) + c_{ph}(\lambda) + c_d(\lambda) + c_g(\lambda)$. Detritus is defined here as the term representing non-pigment containing particles of organic or inorganic origin (e.g., sediment, fecal material, plant and animal fragments, etc.). Gelbstoff (sometimes called yellow matter or gilvin) is the term for optically active colored dissolved organic material (CDOM). The contribution of gelbstoff to scattering is negligible relative to the other terms. The absorption coefficient of pure seawater is well characterized with greater absorption in the red than blue portions of the visible spectrum ([11]; Figure 1). Detrital and gelbstoff absorption spectra tend to decrease monotonically with increasing wavelength and can be modeled using an exponential function (Figure 1). Phytoplankton spectral absorption varies significantly in relation to pigmentation of particular species, community composition, and environmental changes (Figure 1). Characteristic peaks are typically found near wavelengths of 440 nm and 683 nm and are related to chlorophyll-*a*.

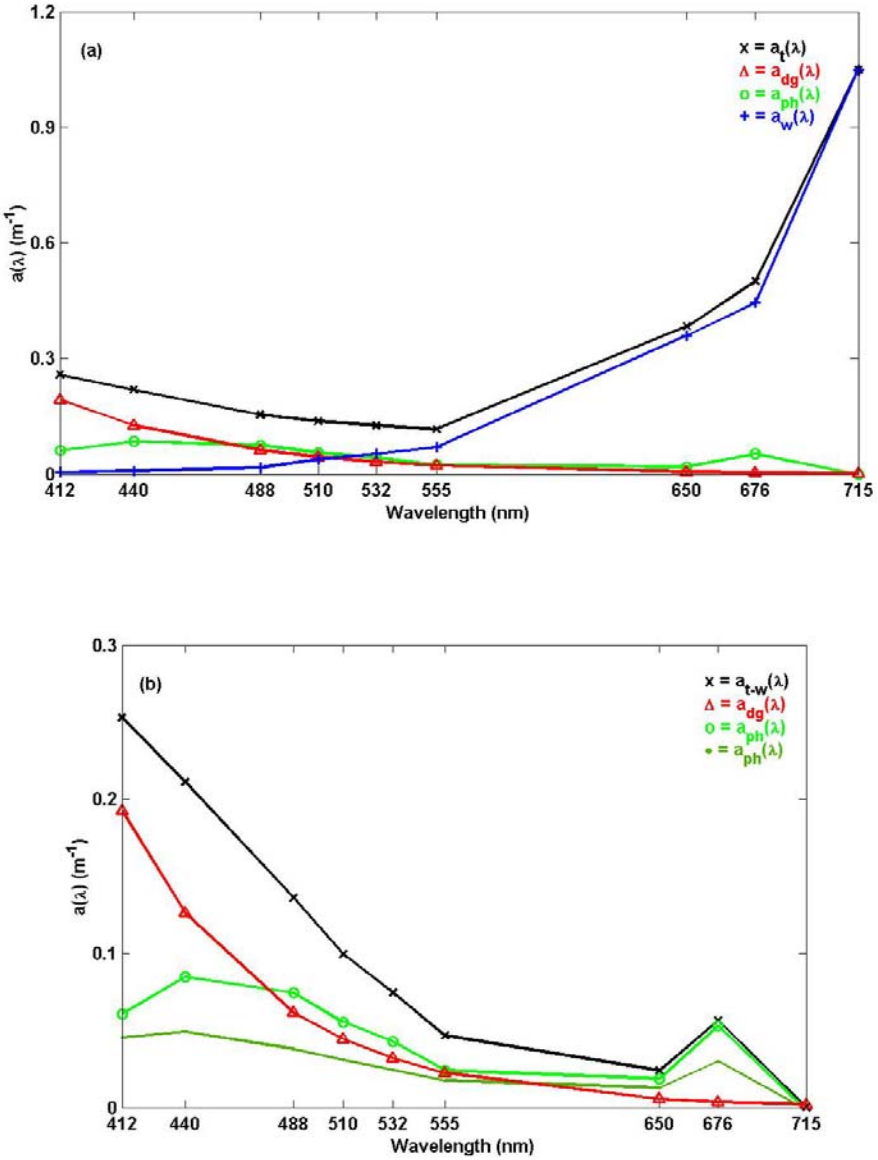

Figure 1. (a) Total spectral absorption (x's), spectral absorption by detritus plus gelbstoff (triangles), spectral absorption of phytoplankton (circles), and spectral absorption due to water (pluses), and (b) an enlargement of (a) showing total spectral absorption minus the contribution by water (x's), spectral absorption by detritus plus gelbstoff (triangles), and spectral absorption of two different species of phytoplankton (circles are dominated by diatoms and dots are dominated by dinoflagellates). The total absorption spectrum was measured by an ac-9 during the Coastal Mixing and Optics experiment and was partitioned into detritus plus gelbstoff and phytoplankton using methods presented in Chang and Dickey ([10]). The water absorption spectrum is from Pope and Fry ([11]).

Quasi-inherent optical properties (quasi-IOPs)

The quasi-inherent optical properties (quasi-IOPs) are the vertical diffuse attenuation coefficients for radiance, $K_L(z, \lambda)$, and irradiance, $K_d(z, \lambda)$, where z is depth. These are defined as the logarithmic derivative of the specified radiometric quantity with respect to depth, e.g., $K_d(z, \lambda) = [1/(z_2 - z_1)] * \ln(E_d(z_1,\lambda) / E_d(z_2,\lambda))$ where z_1 and z_2 are two different depths ([2]). The vertical diffuse attenuation coefficients provide information about vertical change of light intensity through the water column. Quasi-IOPs are those quantities that, strictly speaking, depend on the ambient light field but have been shown to behave similarly to the IOPs. Strong relationships generally exist between $K_d(z, \lambda)$ and $a(\lambda)$. These relationships tend to break down for low sun angles (sunrise and sunset) and when scattering becomes very important (e.g., coccolithophore blooms). $K_d(z, \lambda)$, the vertical diffuse attenuation coefficient of downwelling irradiance, can be separated into the four constituents of sea water (water, phytoplankton, detritus, and gelbstoff), similar to the IOPs defined above ([12,13,14]). $K_d(z, \lambda)$ has the same units (m^{-1}) as the IOPs, $a(\lambda)$, $b(\lambda)$, and $c(\lambda)$. At the same time, $K_d(\lambda)$ is dependent on the angular distribution of the light field since it is defined as a property of the radiation field.

Radiative transfer theory

Radiative transfer theory involves a set of mathematical formulations linking IOPs and the boundary conditions (influenced by the surface radiance distribution, and sea surface and bottom characteristics) to the AOPs of the water column. Radiative transfer theory allows users to predict AOPs given knowledge of environmental forcing conditions and actual measurements or best estimates of IOPs (i.e., forward problem). Conversely, estimates of the IOPs, given remotely sensed water-leaving radiance or remote sensing reflectance, could be made (i.e., inverse problem). Exact relations between inherent and apparent optical properties can be derived from the Gershun equation ([3]). However, these relations can be simplified and validated against numerical solutions to the radiative transfer equation. Gordon et al. ([15]) used Monte Carlo simulations for waters characterized by b/a values ranging from 1.0 to 5.0 to confirm that reflectance, $R(\lambda)$, is a function of $b_b(\lambda)/(a(\lambda) + b_b(\lambda))$ or $b_b(\lambda)/a(\lambda)$. The simple relationships between IOPs and AOPs tend to break down during periods of low sun angle and when highly reflective particles are present ([16,17]).

ADVANCES IN OPTICAL INSTRUMENTATION

The collection of ocean optical data began in the mid-1800's with the Secchi disk, a white disk 25-30 cm in diameter whose depth of disappearance from sight is defined as the Secchi depth. This depth is a rough measure of turbidity or water clarity. Unfortunately, this technique relies on eyesight; thus results change with different observers. Mankovsky et al. ([18]) present a time series of Secchi depth measurements from the Black Sea spanning seven decades from 1922 to 1995. The record shows a decrease in Secchi depth from about 15 to ~8 m from the 1980's to the 1990's. Two possible reasons for this increase in turbidity are (1) an increase in the concentration of highly reflective phytoplankton, called coccolithophores and (2) an increase in CDOM from river discharge into the Black Sea. Falkowski and Wilson ([19]) used a 90-year record of Secchi depth observations in the North Pacific Ocean to determine that small systematic increases in phytoplankton have occurred on the edges of the central ocean gyre, while the gyre core has undergone a small depletion of phytoplankton.

The advancement of *in situ* optical instrumentation saw its largest expansion beginning approximately 30 years ago. One of the first AOP instruments measured broadband scalar irradiance, E_0 or PAR. PAR sensors receive light from approximately 4π steradians and record output voltage with a photodetector (Figure 2). The spherical light collectors are made of diffusing plastic or opal glass. PAR measurements provide important information regarding the light available for phytoplankton. Sensors similar to PAR sensors use flat plate cosine or hemispherical collectors for different measurements or calculations of the AOPs. These are called spectroradiometers, which measure radiance, irradiance, or scalar irradiance (Figure 2). Spectroradiometers use a variable monochromator placed between a light collector and a photodetector ([20]). Radiance sensors are designed to accept light over a small solid angle (typically a viewing angle of a few steradians). Irradiance cosine collectors are designed such that their responses to parallel radiant flux are proportional to the angle between the normal to the collector surface and the direction of the radiant flux. Light separation for a spectral signal is generally achieved by using sets of interference filters (usually 10 nm full bandwidth at half power) selected for specific purposes such as investigating absorption peaks and hinge points for pigment analyses and phytoplankton species identification and chlorophyll estimates. Higher spectral resolution (hyperspectral; < 5 nm continuous resolution from 350 to 800 nm) spectroradiometers have become commercially available in the last 2 years (Figure 2). Hyperspectral resolution is usually achieved by using grating monochromators.

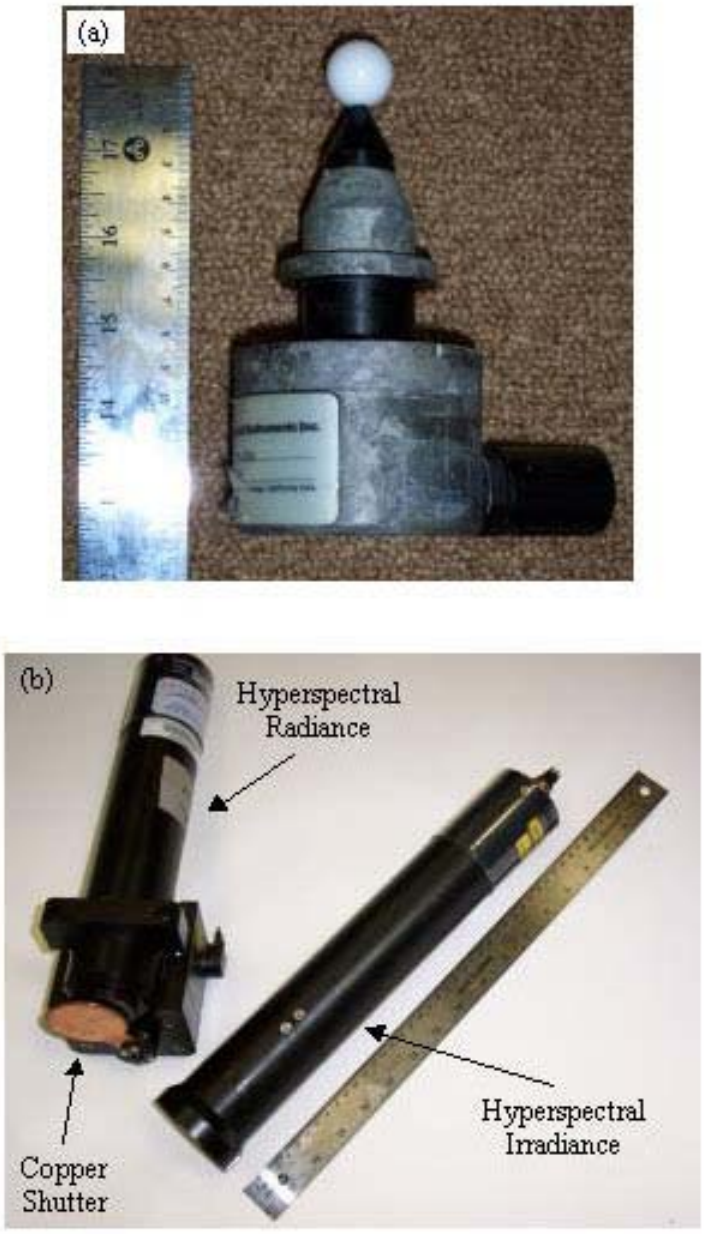

Figure 2. Photographs of instruments that measure apparent optical properties: (a) photosynthetically available radiation (PAR) sensor, (b) hyperspectral radiance sensor with copper anti-biofouling shutter and hyperspectral irradiance sensor.

One of the first IOP sensors for oceanic research was the beam transmissometer ([21]). The beam transmissometer measures the proportion of an emitted beam that is lost through both absorption and scattering. The emitted beam, usually a red light emitting diode (LED; at 660 nm) passes through a pre-determined pathlength to a detector. The wavelength of 660 nm was selected in order to measure particulate attenuation; dissolved matter attenuation is minimal at 660 nm. The beam attenuation coefficient (beam c) is derived from beam transmissometer measurements. Within the past decade, other *in situ* IOP sensors have been developed. Spectral absorption-attenuation meters (ac-meters) have become commercially available since the mid-1990's ([22]; Figure 3). These instruments concurrently measure spectral absorption and attenuation coefficients at up to 100 wavelengths (ac-9 for nine wavelengths, HiStar for 100 wavlengths) for spectral signatures of both particulate and dissolved material. The instrument contains two tubes through which seawater is pumped. The inside of the beam c tube (c-tube) is flat black to minimize reflections whereas the absorption coefficient tube (a-tube) is reflective in order to maximize internal reflection to better estimate absorption. The spectral scattering coefficient can be computed from ac-meter data by simply performing the difference $b(\lambda) = c(\lambda) - a(\lambda)$.

Backscattering can be estimated using instruments that measure scattering over a single fixed angular range at several different wavelengths (Figure 3). The backscattering coefficient estimation is based on scattering theory and statistical relationships relating scattering at a given angle to the integral over the backward direction [23]). Particle size distributions, shapes, and compositions of particles (biological vs. detrital vs. sediment) can be estimated with backscattering properties. *In situ* particle size distributions can also be measured using laser (Fraunhofer) diffraction instruments ([24]). These often employ CCD array photodetectors. Information about particle sizes can also be inferred from measurements of the volume scattering function (VSF). Some new VSF instruments measure at fixed numbers of angles with the functional form being determined using theory and polynomial curve fits ([25,26]). Another new instrument resolves the entire VSF from 0.5 to 179 degrees with an angular resolution of 0.3 degrees ([27]). The total scattering ($b(\lambda)$) and the backscattering coefficient, $b_b(\lambda)$, can then be estimated through direct integration of the measured VSF over the appropriate angular ranges.

Figure 3. Photographs of instruments that measure inherent optical properties: (a) WET Labs, Inc. nine-wavelength absorption-attenuation meter (ac-9), and (b) HOBI Labs six-wavelength backscattering instrument (Hydroscat-6).

Many species of phytoplankton and zooplankton are bioluminescent, meaning that they produce light by a chemical reaction that originates in the organism. These bioluminescent organisms can be detected *in situ* with bioluminescence sensors. These sensors usually pump water through

a baffle, mechanically stimulating the organisms to generate bioluminescence. Optical sensors inside the instrument's chamber then detect the amount of light produced by the organisms. The first generation of bioluminescence sensors were quite large (about the size of an automobile) and could only be utilized as shipboard samplers. Presently, researchers (e.g., J. Case, University of California, Santa Barbara) are developing smaller-scale bioluminescence sensors that can be mounted in AUVs and other autonomous sampling platforms (see below).

New *in situ* chemical measurements have greatly improved with technologies, now utilizing optical (spectrophotometric) methods with reagents to derive high-resolution measurements of environmentally important chemicals, e.g., nitrate, nitrite, phosphate, and iron ([28]). One of the main advantages of these *in situ* optically-based chemical sensors is the ability to integrate timely measurements of ocean chemistry with other oceanographic parameters such as conductivity-temperature-depth (CTD), fluorometers, and other optical sensors. Also, *in situ* chemical sensors are being deployed on different types of sensor packages to resolve chemical processes on several different time and length scales. Challenges with these instruments involve length of deployment, calibration, and storage of reagents. Chemical properties of the water column can also be inferred from analyses of spectral fluorescence. Technologists are currently working on miniaturizing spectral fluorometers for more robust measurements in a multitude of oceanographic settings.

Light sensing devices need unobstructed light paths for accurate optical data. The build up of biological material, i.e., biofouling in the form of bacterial or algal growth or exudates, or growth of higher trophic level species such as barnacles, must be reduced. Useful data from moorings have often been limited to a few weeks in coastal waters ([29]). However, work is progressing to mitigate this problem ([30,31]). Anti-biofouling techniques for optical instruments are necessary, even for short-term deployments in the coastal ocean ([30,31]). Presently used techniques often involve the use of copper and are essential for long-term deployments of optical sensors. Copper significantly reduces marine fouling for optical sensor deployments in the coastal ocean and can effectively replace previously used highly toxic chemical anti-foulants, e.g., tributyl tin (TBT), bromine, and chlorine ([31]). Copper shutters that open during sampling and close over radiometric sensors, fluorometers, and other optical windows during idle periods, can significantly reduce biofouling of optical instruments (Figure 2). These anti-biofouling methods have been shown to increase instrument deployment times from ~1 month to as long as 4 months in the coastal ocean (see Chang and Dickey [32] and Chang et al. [33]).

OPTICAL METHODS FOR COASTAL OCEAN RESEARCH

Improved understanding of coastal ocean processes is essential since the majority of the world's primary production occurs on continental shelves and the coastal ocean is most utilized and impacted by humans. Coastal ocean research is difficult because physical, chemical, and biological processes in the coastal ocean are generally more dynamic and complex than in the open ocean. Coastal ocean processes are affected by boundary conditions not observed in the open ocean. Physical, chemical, and biological processes interact with the ocean bottom through deposition, accumulation, and resuspension of biological or detrital material, and nutrients. The presence of a lateral boundary, i.e., coastline, can contribute to upwelling and amplify tidal

forces and waves, and hence turbulence, affecting particle concentration, characteristics, and distribution, and phytoplankton diversity. Freshwater inputs through river and estuarine flows can influence stratification and hydrography, which have been shown to greatly affect chemical, biological, and geological processes. In addition, coastal ocean processes are nonlinear and often interact with each other, resulting in cascades of energy to several different temporal and spatial scales (Figure 4).

Coastal ocean sensor platforms

Coastal ocean research must incorporate interdisciplinary sensors and systems capable of sampling on multiple and appropriate time and space scales relevant to physical, biological, chemical, and geological processes (Figure 4, modified after Dickey [34]). The utilization of a variety of complementary ocean observing platforms can greatly improve our knowledge of coastal ocean ecology and health of the ocean. Multiple platforms are necessary because of specific platform advantages and limitations, as discussed below.

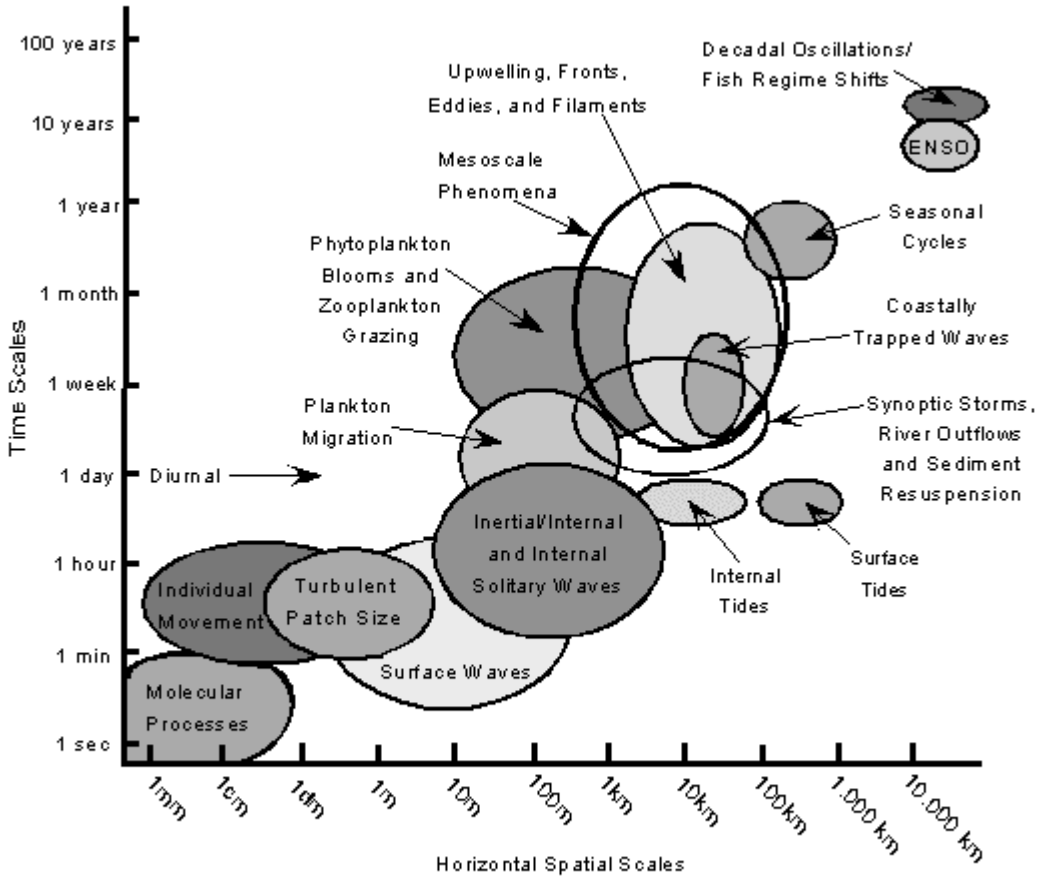

Figure 4. Schematic diagram of temporal and horizontal spatial scales of processes in the coastal ocean.

Remote sensing

Optical remote sensing technology came of age with the satellite-borne Coastal Zone Color Scanner (CZCS), which provided global ocean color data from 1978 until its demise in 1986. In 1996 and 1997, remotely sensed ocean color data were again available from two improved ocean color sensing satellite systems: (1) Ocean Color and Temperature Scanner (OCTS, Japan) and (2) Sea-viewing Wide Field-of-view Sensor (SeaWiFS, United States). At present there are fourteen ocean color satellites in operation and two more are planned for deployment in 2005 and 2007. These ocean color satellites are considered as medium-resolution, multispectral; spectral coverage ranges from 375 nm into the infrared, at multiple wavebands (between 4 and 36). The spatial resolution of these current satellites ranges from 250 m to 1.2 km. Recently, the development and use of hyperspectral (< 5 nm resolution in the visible and into the infrared wavelengths) remote ocean color sensors has increased, particularly for coastal ocean research. Hyperspectral remote sensors are generally deployed on aircraft for spatial resolution of tens of meters.

Remotely sensed measurements of oceanic optical properties from satellites and aircraft involve observations that rely on the Sun for illumination of the ocean surface. The instruments are commonly spectroradiometers that measure the radiance entering the aperture of the sensor. A variety of scanning mechanisms are utilized to generate two-dimensional fields or images to provide nearly synoptic optical observations over the oceans ([35]; Figure 5). The interpretation and quantification of remotely sensed data can be severely limited. Several correction factors are necessary to overcome the complications from the specular reflection off of the sea surface in the form of Sun glint, the high degree of variability in atmospheric scattering and absorption, and the bi-directionality of both the downwelling and the upwelling radiance distributions. In addition, the surface downwelling irradiance must be measured or estimated to generate the normalization necessary to compare different oceans at different times in a quantitatively meaningful way. Cloud cover and coastal fog often obscure remote sensors, limiting the usefulness of images and data for analyses. Most importantly, remote sensing data are limited to the upper optical depth of the ocean ([36]), typically < 1 m in coastal waters. Satellite remote sensing temporal and spatial coverage is severely restricted according to the nature of satellite orbital mechanics and illumination and viewing geometries. Ocean color images are typically available once or twice per day for a particular region of interest. Aircraft remote sensors are constrained in terms of spatial coverage and deployment time period. Thus, satellite and aircraft information must be complemented with *in situ* observations to calibrate remote sensors, provide continuous time series, and to characterize important vertical structure of ocean optical properties.

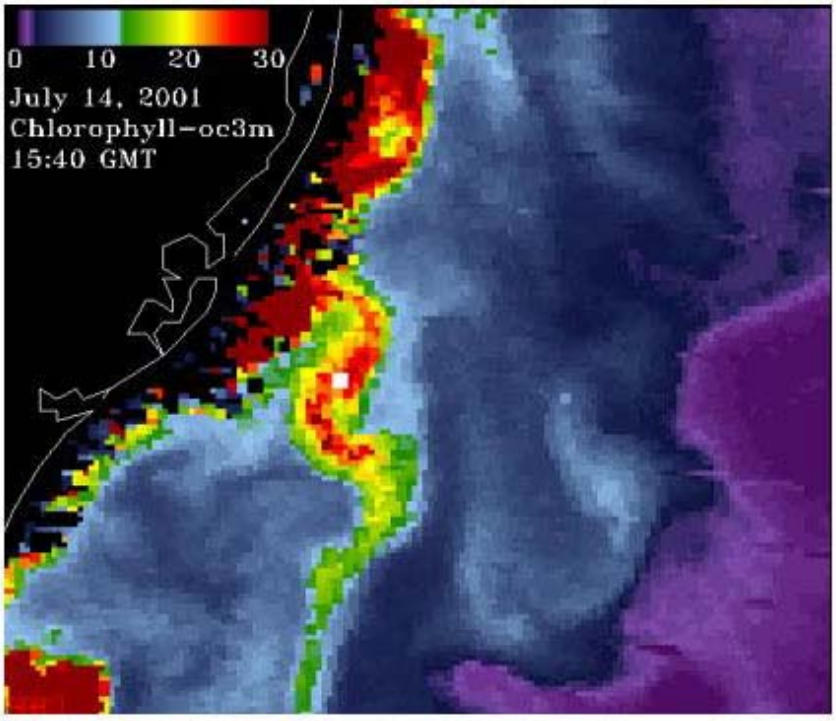

Figure 5. Example of an ocean color satellite image taken by Moderate Resolution Imaging Spectroradiometer (MODIS) off the coast of New Jersey in summer 2001. A high biomass filament is visible near the center of the image. The white square represents the location of our nearshore coastal mooring, deployed during the Hyperspectral Coastal Ocean Dynamics Experiment (HyCODE). (Image courtesy of Rick Gould and Bob Arnone.)

Ships

Ship sampling is a valuable resource for coastal ocean research if utilized in conjunction with modern, autonomous sampling platforms. Ship sampling provides: 1) detailed process-oriented measurements for specific research studies and 2) nearly continuous data with depth and over long distances. Ship sampling may include on-station vertical profiling of instruments and instrument packages; on-station and underway ship-mounted, tethered, or hand-held radiometric measurements; and underway sampling using flow-through systems ([37]), towed undulating ([38]), and fixed depth bodies that act as instrument platforms. One of the advantages of ship sampling is that calibrations and cleaning of optical instruments can be performed between each profile or deployment to provide accurate, freshly calibrated, essentially non-biofouled data. A second advantage of ships is that advanced analytical instrumentation that cannot be deployed from *in situ* platforms can be utilized, e.g., molecular probes, mass spectrometers, 'clean' methods for ocean chemistry, and radioactivity measurement systems. In addition, ships remain the only practical platforms capable of collecting water samples and net tows for laboratory

chemical and biological analyses. Ships have limitations in terms of their high cost, limited availability, and restricted synopticity in sampling. Also, they are constrained by meteorological and sea-state conditions.

Autonomous Underwater Vehicles (AUVs), Remotely Operated Vehicles (ROVs), and Gliders
Recently, numerous programs have begun to exploit autonomous underwater vehicles (AUVs), remotely operated vehicles (ROVs), and gliders for coastal ocean scientific studies ([39]). A description of the history, and present and future capabilities of AUVs is provided by Griffiths et al. ([40]). Modern capabilities of AUVs and ROVs have become possible because of the development of new oceanographic sensors and systems that are relatively small in size and consume low to moderate power. Some of the advantages of autonomous platforms include low cost per deployment, potential to sample in environments generally inaccessible to ships, good spatial coverage and sampling over repeated sections, capability of feature-based or adaptive sampling, and ability for deployment of several vehicles from moorings, ships, offshore platforms, and coastal stations. The primary disadvantage of AUVs is related to their power consumption. AUVs must be recharged regularly and hence, cannot be used for long-term deployments without a docking station. The glider concept uses variable buoyancy control, lift surfaces (wings), a hydrodynamic shape, and trajectory control using internal moving mass to control its motion and therefore does not draw as much power as an AUV. With typical forward speeds of 0.25 m s^{-1}, gliders may be used as long-term virtual moorings for time series in one location or for long transects.

Moorings and Bottom Tripods
Studies of environmental changes in the coastal ocean on timescales from minutes to decades can be achieved by the use of moorings and bottom tripods. An increasing number of optical, chemical, biological, and physical parameters are being measured from these platforms at multiple depths. A great advantage of moorings and tripods is the ability to sample during times of inclement weather and high sea-states. One of the limiting factors for these types of platforms is the large size and weight of moorings and the high cost of development and deployment. The greatest disadvantage of these platforms is biofouling of sensors ([30,31]). Additional future technological advances will allow measurement systems to be more compact and lightweight, less power-hungry, and lower in cost. These can be achieved through the development of micromachines, microelectromechanical systems (MEMS), miniature lasers and optical components, fiber-optics, and nanotechnology ([28,41,42]). Bottom tripods and their instrumentation may be placed in virtually the same environments as moorings using similar suites of sensors and samplers deployable from moorings. Data telemetry and the use of moored cabled networks can provide researchers with oceanographic time series data in real-time or near real-time.

Data synthesis and analysis
Optical data provide valuable information regarding biology, chemistry, geology, and physics of the coastal ocean. Past coastal ocean interdisciplinary programs have focused on the use of optics to investigate carbon fluxes, benthic processes, mixing processes, thin layers, upwelling, mesoscale features, harmful algal blooms, and satellite algorithm development (see review by Dickey and Chang [43]).

One of the most valuable aspects of optical oceanography is the ability to identify water column constituents using commercially available *in situ* optical instrumentation and relatively simple data analysis methods. Qualitative estimates of particle type can be made using property-property plots of chlorophyll fluorescence against beam attenuation data (Figure 6). High chlorophyll values with relatively low beam attenuation values are indicative of biological material, whereas high beam attenuation values with relatively low chlorophyll values imply detrital matter (defined as all non-living matter such as sediment, dead organic matter, etc.). A quantitative method for distinguishing water column constituents is partitioning of total spectral absorption using *in situ* measurements and models (e.g. : [8,9,10,44]). The ac-9 and HiStar measure total spectral absorption minus the contribution by pure water (the pure water spectrum is well known; [11]). This quantity can be separated into the major absorbing components of seawater: CDOM and particulates, further partitioned into components of detritus and phytoplankton ($a_t(\lambda) = a_w(\lambda) + a_{ph}(\lambda) + a_d(\lambda) + a_g(\lambda)$; Figure 1). Spectral and hyperspectral phytoplankton absorption data can be used with fourth derivative analysis to identify dominant pigment peaks in absorption and thus, phytoplankton species by group ([45,46,47,48]). Bioluminescence data can be used as an indicator of bioluminescent dinoflagellates and zooplankton.

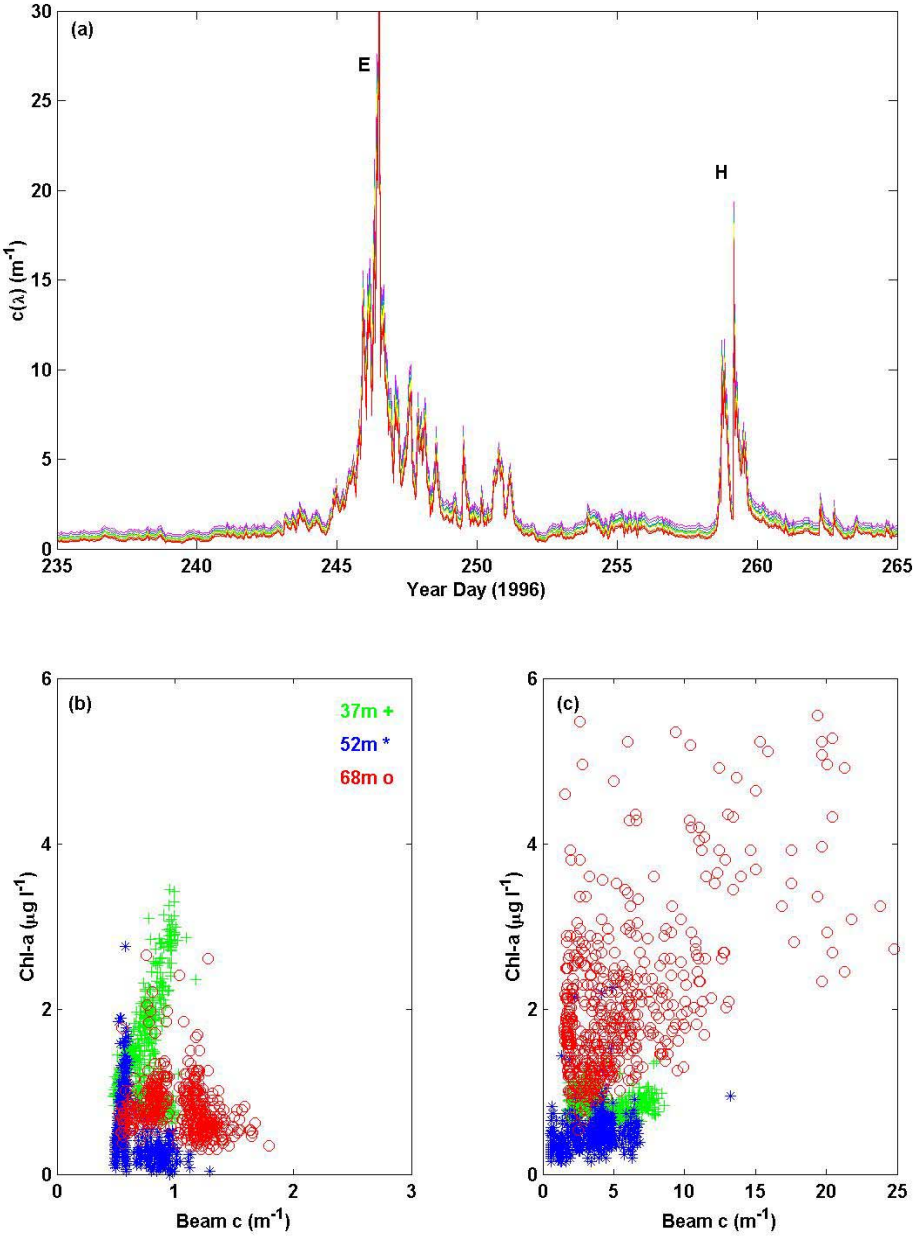

Figure 6. (a) Time series of beam attenuation coefficient collected by an ac-9 deployed on a bottom tripod during the Coastal Mixing and Optics experiment. 'E' and 'H' represent times of passages of Hurricanes Edouard and Hortense. Property-property plots of chlorophyll-a concentration (measured by a fluorometer) versus beam attenuation used to qualitatively distinguish between particle types for (b) year days 239-241 (prior to hurricanes) and (c) year days 246-248 (during Hurricane Edouard passage).

Beam c data and simple linear algorithms can provide estimates of particulate concentrations, suspended sediment volume, concentrations of particulate organic carbon (POC) and productivity in the form of POC, and thus carbon flux (e.g. : [49,50]). In addition, the shape of spectral beam c can give information about the particle size distribution; flatter attenuation spectra denote a flatter particle size distribution while steeper attenuation spectra indicate a steeper particle size distribution ([51]). Recent studies have begun to utilize the backscattering ratio, $b_b(\lambda)/b(\lambda)$, to estimate bulk particle composition ([52,53]). Relatively low values of $b_b(\lambda)/b(\lambda)$ are consistent with low refractive index particles such as organic material and higher $b_b(\lambda)/b(\lambda)$ indicates high refractive index particles such as inorganic material. Twardowski et al. ([52]) developed a quantitative model to calculate the index of refraction of an ensemble of particles given the backscattering ratio, based on Mie theory.

Spectral fluorescence data can be utilized with excitation-emission matrix spectroscopy (EEMS) to provide information about hydrocarbons, humic and fulvic acids associated with CDOM formation, and other characteristics of CDOM, including separation between freshwater and seawater sources ([54]). Petrenko et al. ([55]) used spectral fluorescence data to investigate optical characteristics of sewage plume waters in Mamala Bay, HI. Their results confirmed that certain sets of excitation and emission wavelengths (e.g., Ex/Em = 228 nm/340 nm; [55]) could be used to distinguish between sewage plume and ambient waters. These results are significant for the future design and monitoring of industrial and sewage outfall plumes in heavily populated coastal areas.

Remotely sensed ocean color data are used to infer concentrations of biological quantities (chlorophyll, biomass, and primary productivity; [35,56,57]) and optical information (absorption and backscattering coefficients) synoptically. Ocean color algorithms have been developed to quantify constituents in the water column using wavelength or waveband ratios. Different ratios are employed for different optical parameters, e.g., water-leaving radiance at 490 to 555 nm ($L_{wn}(490)/ L_{wn}(555)$) for chlorophyll-*a* concentration and $L_{wn}(443)/L_{wn}(510)$ for CDOM ([58]). A review by O'Reilly et al. ([56]) presents several different chlorophyll-*a* algorithms that apply different wavelengths ratios depending on open ocean water column characteristics. Coastal ocean algorithms to determine chlorophyll-*a* concentrations and spectral absorption and backscattering have been developed (e.g. : [59,60,61]). Gould and Arnone ([62]) formulated algorithms to quantify salinity and total suspended solids from ocean color data. The algorithms assumed an inverse correlation between absorption at 412 nm and salinity and a positive correlation between total suspended solids and backscattering at 555 nm. Their results, although specific for very nearshore regions, are promising for future derivation of physical and geological parameters and for tracking water mass movements using remotely sensed ocean color images. Newly developed multispectral and hyperspectral remote sensors allow the use of a single instrument to provide several to a multitude of wavelengths and wavelength ratios to more accurately resolve a wider variety of water column constituents and resolve bottom bathymetry ([63]). Species identification is now possible using hyperspectral radiometric measurements ([64]); phytoplankton pigment peaks to classify phytoplankton taxa are strongly defined in hyperspectral ocean color data. Passive solar fluorescence (near peak at 685 nm) measurements show great promise for chlorophyll estimates in the coastal ocean ([6,7,65,66,67,68]).

Optical methods to identify phytoplankton species are extremely valuable tools for harmful algal bloom (HAB) research. Ecological concerns regarding HABs in the coastal ocean have been increasing in recent years because of negative impacts on the fish and shellfish industry, aquaculture industry, tourism industry, marine mammals and birds, recreation, and human health. Moored optical systems can be utilized for detection, monitoring, and assessment of HABs. Johnsen and Sakshaug ([69]) describe a HAB monitoring program along the Norwegian coast that utilizes a network of buoys that employ bio-optical, biological, chemical, and physical instrumentation. When a potential bloom is detected by the buoy system, i.e., when certain properties exceed pre-specified threshold values, an observer network, consisting of local fish farmers and Norwegian Food Hygiene Control Authorities, is informed. Then, detailed sampling is conducted to determine the species and potential toxicity of the bloom. This monitoring program has proven useful for advanced public warning of HABs occurring along the entire Norwegian coast. The feasibility of moored optical detection systems for HAB monitoring and research has also been discussed by Cullen et al. ([70]) and Schofield et al. ([71]). Scientists are currently working on remote detection of HABs using satellite ocean color imagery ([64,72]).

Ocean optics researchers are also investigating the use of optics for water mass characterization and hence, tracers. Many mesoscale features in the coastal ocean exhibit strong optical or bio-optical signatures that are different from surrounding waters. A subsurface coastal jet was identified using optical data collected from a nearshore profiling mooring during the Hyperspectral Coastal Ocean Dynamics Experiment (HyCODE) in 5 m of water off the coast of New Jersey ([33]). The nearshore jet, originating from an upwelling center to the north, was relatively clear compared to the highly turbid nearshore waters and could easily be seen in optical data. This jet often forms along the U.S. east coast during upwelling conditions in the summer. Just south of the HyCODE site, bottom topography (sand bars) directs the jet offshore, resulting in a counterclockwise eddy that extends to the shelf break. The high velocity of the jet can resuspend sediment from the sand bars, entraining particulates into the eddy. This turbid eddy displaces clearer waters offshore and can sometimes be seen from satellite ocean color images.

Optical data can be coupled with complementary hydrographic data to track river plumes in the coastal ocean ([62]). Salinity and CDOM absorption at the blue wavelengths (e.g., $a_g(412)$) are oftentimes coherent (180° phase) during freshwater flushing events (river or estuarine flow). A mid-shelf mooring was deployed during HyCODE in 25 m water depth in summer 2000. Three pulses of the Hudson River plume can be seen in $a_g(412)$ and salinity data from May to June 2000 (Figure 7). This plume is also visible in remotely sensed optical data. Figure 7 shows that remote sensing reflectance can be utilized to track river plumes; the ratio $R_{rs}(550)/R_{rs}(400)$ is significantly coherent with $a_g(412)$ and not coherent with other optical quantities (chlorophyll-*a* shown).

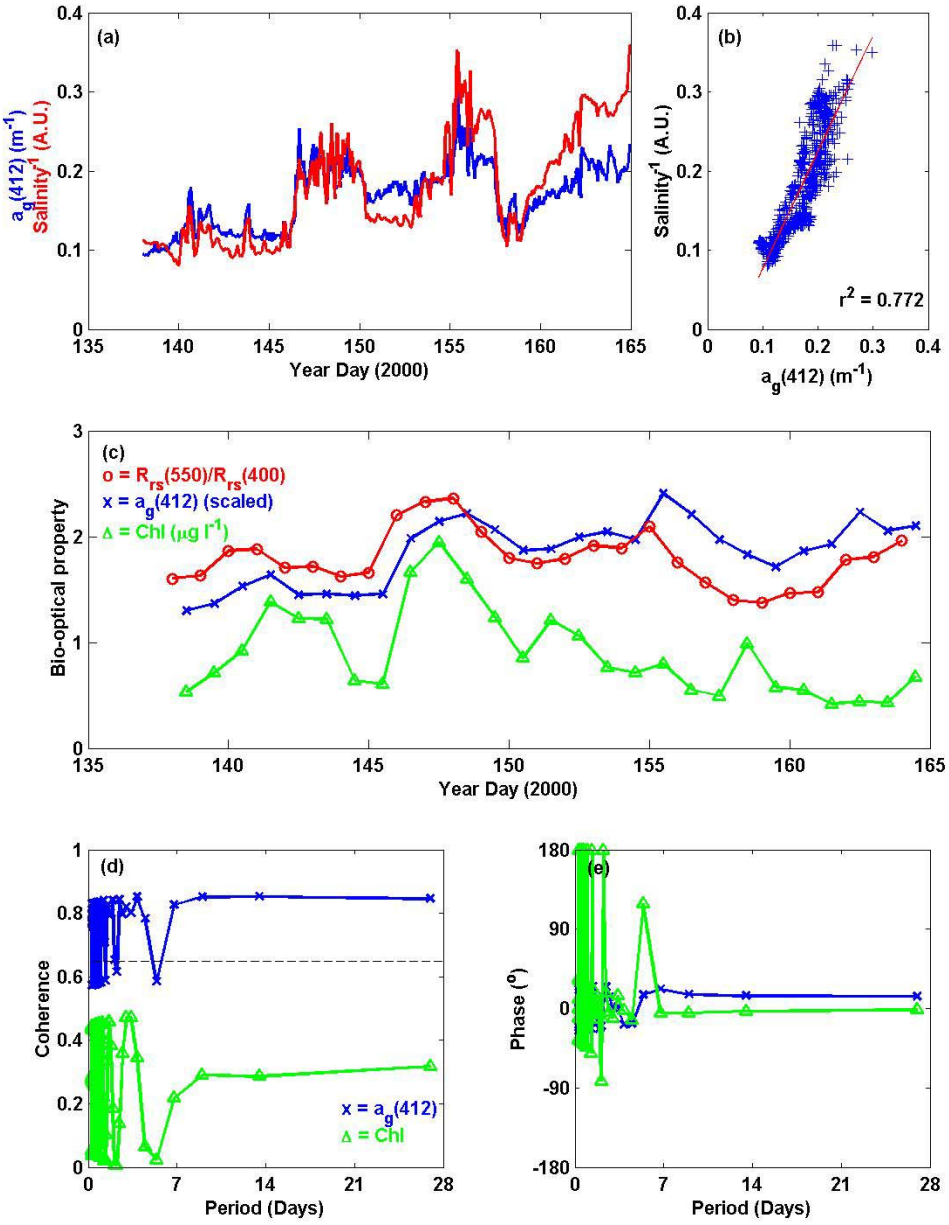

Figure 7. (a) Time series of gelbstoff absorption at 412 nm ($a_g(412)$; measured by an ac-9 and partitioned using the model presented in Chang and Dickey ([10])) and salinity^{-1}, (b) scatterplot of $a_g(412)$ versus salinity^{-1} with linear regression, (c) time series of the ratio of remote sensing reflectance at 550 nm to 400 nm ($R_{rs}(550)/R_{rs}(400)$; circles), $a_g(412)$ (x's), and chlorophyll-a concentration measured by a fluorometer (triangles), (d) coherence and (e) phase between $R_{rs}(550)/R_{rs}(400)$ with $a_g(412)$ (x's) and $R_{rs}(550)/R_{rs}(400)$ with chlorophyll-a concentration (triangles). The dashed line represents statistical significance.

Several investigators have utilized optical data to study internal waves. Weidemann et al. ([73]) found that internal solitary waves (ISWs) can vertically modulate water column IOPs and can be seen in remotely sensed optical data. They hypothesize that the ISW signals are generated by changes in upwelling radiances from the interior of the water column and not by changes in surface reflectance. These findings are significant as internal waves can cause vertical movement of phytoplankton and nutrients into or out of the euphotic layer, affecting primary production, and can also resuspend and/or transport sediment ([74]). Results from a study in shallow waters off Oceanside, California revealed that spikes in optical attenuation, observed using ac-9s deployed on near-bottom moorings, were associated with the trailing edges of ISWs ([75]). The near-bottom increases in beam c were correlated with bottom convergent currents formed by ISWs and not correlated with high bottom shear stress. Bogucki et al. ([76]) found similar increases in near-bottom beam c during the passages of ISWs off Los Angeles, California. They concluded that the leading wave of the ISW packet resulted in flow separation/instability and sediment resuspension, i.e., a virtual sediment pump mechanism.

Many other benthic processes have been studied and monitored using optical instrumentation deployed on bottom tripods in the coastal ocean. Sediment and detrital resuspension and settling, bedform formation and movement, bioturbation, and flocculation/deflocculation of organic particles have been investigated on the California coast, the Mid-Atlantic Bight, and in the Gulf of California ([77,78,79]). The burial of pollutants from industrial activity and sewage outfalls accentuates the importance of understanding and predicting sediment movement in the coastal ocean. The Sediment TRansport Events on Shelves and Slopes (STRESS) program was conducted on the northern California coast to investigate processes controlling sediment transport and to develop models to predict these processes ([77]). Optical backscatterance sensors, beam transmissometers, an optical settling box, a stereocamera for photographs of bed conditions, and laser *in situ* settling tubes were mounted on bottom tripods just offshore of the Russian River outflow. Using these optical instruments, STRESS scientists were able to successfully resolve small-scale bed topography and estimate particle concentrations, sizes, and settling velocity to develop models for prediction of sediment resuspension and transport.

Sediment resuspension by hurricanes and storms has also been observed using optical instrumentation deployed on bottom tripods and moorings. Within two weeks in summer 1996, two category 4 hurricanes, Edouard and Hortense, passed over the Coastal Mixing and Optics (CMO) experiment site, located in the Mid-Atlantic Bight, about 120 km south of Cape Cod, Massachusetts, in 70 m water depth. Data from physical (current meters) and optical (ac-9s and fluorometers) instrumentation showed that intense winds and hurricane-associated currents and waves resulted in resuspension of detrital material and relict pigments ([78,80]). Detrital material was distinguished from other types of particles using partitioned spectral absorption data and relict pigments were identified in chlorophyll fluorescence data. Beam c data from the bottom tripod (68 m; 2 m above the bottom) increased from values of nearly 1 m^{-1} to greater than 30 m^{-1} during the passage of Hurricane Edouard, providing further evidence for increased sediment concentrations (Figure 6). Data from ac-9s deployed on a nearby mooring indicated that beam c values increased from 0.2 m^{-1} to greater than 5 m^{-1} at the 52 m depth, and from 0.2 m^{-1} to greater than 2 m^{-1} at 37 m during the passage of Hurricane Edouard (Figure 6). This suggests that sediment was resuspended more than 30 m up into the water column. The increase in beam c is seen first at 68 m, then a half-day later at 52 m, and an additional half-day later at 37

m (Figure 6). The relaxation of sediment concentration (as indicated by beam c) to pre-Edouard conditions occurred at about the same time at all depths (8 September 1996; Figure 6). This implies that the resuspended sediment was advected past the mooring site following the passage of the storm. Volume concentration data and photographic results obtained by optical instruments on the bottom tripod reveal that high levels of bottom and near-bottom turbulence due to Hurricanes Edouard and Hortense produced high concentrations of smaller, less dense particles due to the break-up of flocculates ([79,80,81]). The large particles (flocs) then reappeared several hours following the passage of the hurricanes when the intensity of turbulence weakened.

Quantification of temporal and spatial scales of bio-optical variability and decorrelation scales has been accomplished using optical instruments (as described above) deployed on moorings and drifters, and profiled from ships ([32,33,82]). Decorrelation analyses using shipboard transects along the New Jersey coast in less than 25 m of water during HyCODE have revealed the presence of an extensive coastal turbidity front that separated highly turbid (high concentrations of particulates) nearshore waters from relatively clear offshore waters. Small-scale (order of a few km) fronts were also identified along this transect, occurring on both the inshore and offshore sides of the turbidity front. These small-scale fronts were controlled by the semi-diurnal tides and acted to converge and diverge nutrients, particles, and thus biological material ([33]). The dominant scales of temporal variability in the coastal ocean have been attributed to diurnal and semi-diurnal tides, diel, seasonal, and inertial frequencies during storms, as determined by spectral frequency analyses during HyCODE and the CMO experiment ([32]). Episodic events, such as those described above, often interrupt these cycles and greatly affect coastal ocean physical, biological, chemical, and geological processes.

SUMMARY AND CONCLUSIONS

Ocean optics provides valuable tools for understanding physical, biological, chemical, and geological processes in the coastal ocean. The coastal ocean is considerably more complex than the open ocean due to bottom and coastal boundary effects not significant for open ocean processes. Also, there is greater diversity of organisms, and time and space scales of variability are shorter in the coastal ocean. Progress in coastal ocean research will be enhanced with optical instrumentation deployed on a diverse set of observing platforms coupled with data assimilation and ecosystem modeling efforts. Some of the promising observational tools include: 1) new optical, bio-optical, and optically-based chemical sensors, 2) hyperspectral optical instrumentation that can be deployed from *in situ* platforms, aircraft, and satellites, and 3) several new observing platforms including satellites, AUVs, gliders, and profiling floats and moorings.

As novel optical instrumentation and data collection methods are developed and implemented, optical data syntheses and analyses will be improved and expanded. Autonomous ocean observing platforms will be used to collect interdisciplinary data to advance studies of coastal ocean ecology including health of the ocean (e.g., harmful algal blooms and pollutant dispersal), the carbon budget, parameters affecting and affected by the heat budget, and global warming. Ocean optics is crucial to these efforts as optical data provide essential information about particulate concentration, type, and size distribution, primary production, and water column

turbidity. In addition, optical data can be correlated with complementary physical, biological, chemical, and geological data to identify and track water mass movements in the coastal ocean. Most importantly, optical research methods can be performed with commercially available instrumentation and relatively simple algorithms and models.

ACKNOWLEDGEMENTS

Our work has benefited greatly from collaborations with colleagues. Support for our research has been provided by the U.S. Office of Naval Research, National Science Foundation, National Oceanographic Partnership Program, National Aeronautics and Space Administration, Sea Grant Program, State of Hawaii, Los Angeles County, and the University of California at Santa Barbara.

REFERENCES

1. Jerlov, N. G. 1976, Marine Optics, Elsevier, Amsterdam, Netherlands, 231 pp.
2. Kirk, J. T. O. 1994, *Light and Photosynthesis in Aquatic Ecosystems*, Cambridge University Press, second ed., Cambridge, UK, 509 pp.
3. Mobley, C. D. 1994, Light and Water: Radiative Transfer in Natural Waters, Academic Press, San Diego, CA, 592 pp.
4. Maffione, R. A. 2001, Oceanography, 14, 9-14.
5. Dickey, T., Lewis, M., and Chang, G. 2003, Bio-optical oceanography: Recent advances and future directions using global remote sensing and *in situ* observations, Rev. Geophys., submitted.
6. IOCCG Report Number 2, 1999, Reports of the International Ocean Colour Coordinating Committee, J. Yoder (Ed.), International Ocean Colour Coordinating Group, McNabb Print, Dartmouth, Nova Scotia, Canada, 43 pp.
7. IOCCG Report Number 3, 2000, Reports of the International Ocean Colour Coordinating Committee, S. Sathyendranath (Ed.), International Ocean Colour Coordinating Group, McNabb Print, Dartmouth, Nova Scotia, Canada, 140 pp.
8. Roesler, C. S., Perry, M. J., and Carder, K. L. 1989, Limnol. Oceanogr., 34, 1510-1523.
9. Bricaud A. and Stramski, D. 1990, Limnol. Oceanogr., 35, 562-582.
10. Chang, G. C. and Dickey, T. D. 1999, App. Opt., 38, 3876-3887.
11. Pope, R. M. and Fry, E. S. 1997, Appl. Opt., 37, 8710-8723.
12. Morel, A. 1988, J. Geophys. Res., 93, 10,749-10,768.
13. Gordon, H. R., Brown, O., Evans, R. H., Brown, J. W., Smith, R. C., Baker, K. S., and Clark, D. K. 1988, J. Geophys. Res., 93, 10,909-10,924.
14. Morel, A. and Maritorena, S. 2001, J. Geophys. Res., 106, 7163-7180.
15. Gordon, H. R., Brown, O. B., and Jacobs, M. M. 1975, Appl. Opt., 14, 417-427.
16. Stramska, M. and Frye, D. 1997, J. Geophys. Res., 102, 15,679-15,697.
17. Zheng, X., Dickey, T., and Chang, G. 2002, Appl. Opt., 41, 6477-6488.
18. Mankovsky, V. I., Vladimirov, V. L., Solov'ev, M. V., and Besiktepe, S. T. 1998, Ecosystem Modeling as a Tool for the Black Sea, vol. 2, L. I. Ivanov, and T. Oguz, Kluwer (Eds.), Academic Publishers, Dordrecht, 145-161.

19. Falkowski, P. G. and Wilson, C. 1992, Nature, 358, 741-743.
20. Smith, R. C., Booth, C. R., and Star, J. L. 1984, Appl. Opt., 23, 2791-2797.
21. Bartz, R., Zaneveld, J. R. V., and Pak, H. 1978, SPIE, vol. 160, Ocean Optics V, 102-108.
22. Moore, C. C., Zaneveld, J. R. V., and Kitchen, J. C. 1992, SPIE, 1750, Ocean Optics XI, 330-337.
23. Maffione, R. A. and Dana, D. R. 1997, Appl. Opt., 36, 6057-6067.
24. Agrawal, Y. C. and Pottsmith, H. C. 1994, Cont. Shelf Res., 14, 1101-1121.
25. Dana, D. R. and Maffione, R. A. 2000, HydroBeta: a new instrument for measuring in-situ profiles of the volume scattering function from 10 to 170 degrees, Proceedings from Ocean Optics XV, Monte Carlo, Monaco, CD-ROM.
26. Moore, C., Twardowski, M. S., and Zaneveld, J. R. V. 2000, The EcoVSF – a sensor for determination of the volume scattering function, Proceedings from Ocean Optics XV, Monte Carlo, Monaco, CD-ROM.
27. Lee M. E. and Lewis, M. R. 2003, A new method for the measurement of the optical volume scattering function in the upper ocean, J. Atmos. Ocean Tech., in press.
28. Tokar, J. and Dickey, T. 2000, Chemical Sensors in Oceanography, M. Varney (Ed.), Gordon and Breach Scientific Publishers, Amsterdam, Netherlands, 303-329.
29. Davis, R. F., Stabeno, P., and Cullen, J. J. 2000, Use of bio-optical measurements from moorings to detect coccolithophore blooms in the Bering Sea, Proceedings from Ocean Optics XV, Monte Carlo, Monaco, CD-ROM.
30. Chavez, F. P., Wright, D., Herlien, R., Kelley, M., Shane, F., and Strutton, P. G. 2000, J. Atmos. Ocean. Tech., 17, 215-219.
31. Manov, D. V., Chang, G. C., and Dickey, T. D. 2003, Methods for reducing biofouling of moored optical sensors, *J. Atmos. Ocean. Tech.*, submitted.
32. Chang, G. C., and Dickey, T. D. 2001, J. Geophys. Res., 106, 9435-9453.
33. Chang, G. C., Dickey, T. D., Schofield, O. M., Weidemann, A. D., Boss, E., Pegau, W. S., Moline, M., and Glenn, S. M. 2002, J. Geophys. Res., 107, 3133, doi: 10.1029/2001JC001018.
34. Dickey, T. 2003, J. Mar. Syst., 400, 1-44.
35. Yoder, J. A., Moore, J. K., and Swift, R. N. 2001, Oceanography, 14, 33-40.
36. Gordon, H. R. and McCluney, W. R. 1975, Appl. Opt., 14, 413-416.
37. Balch, W. M., Drapeau, D. T., Fritz, J. J., Bowler, B. C., and Nolan, J. 2001, Deep-Sea Res. I, 48, 2423-2452.
38. Barth, J. A., Bogucki, D., Pierce, S. D., and Kosro, P. M. 1998, Geophys. Res. Lett., 25, 2761-2764.
39. Yu, X., Dickey, T., Bellingham, J., Manov, D., and Streitlen, K. 2002, Cont. Shelf Res., 22, 2225-2245.
40. Griffiths, G., Davis, R., Eriksen, C., Frye, D., Marchand, P., and Dickey, T. 2001, Observing the Ocean for Climate in the 21st Century, C. J. Koblinsky and N. R. Smith (Eds.), GODAE, Bureau of Meteorology, Australia, Melbourne, Australia, 324-338.
41. Kaku, M. 1997, Visions: How Science Will Revolutionize the 21st Century? Anchor Books Doubleday, New York, 403 pp.
42. Bishop, D., Gammel, P., and Giles, C. R. 2001, Physics Today, 54, 38-44.
43. Dickey, T. and Chang, G. 2001, Oceanography, 14, 15-29.
44. Gallegos, C. L. and Neale, P. J. 2002, Appl. Opt., 41, 4220-4233.
45. Millie, D. F., Kirkpatrick, G. J., and Vinyard, B. T. 1995, Mar. Ecol. Prog. Ser., 120, 65-75.

46. Millie, D. F., Schofield, O. M., Kirkpatrick, G. J., Johnsen, G., Tester, P. A., and Vinyard, B. T. 1997, Limnol. Oceanogr., 42, 1240-1251.
47. Prézelin, B. B. and Nelson, N. B. 1997, Plant Metabolism, D. T. Dennis, D. H. Turpin, D. D. Lefebvre, and D. B. Layzell (Eds.), 2nd edition, Longman Scientific and Technical, Essex, England, 274-285.
48. Kirkpatrick, G. J., Millie, D. F., Moline, M. A., and Schofield, O. 2000, Limnol. Oceanogr., 45, 467-471.
49. Siegel, D. A., Dickey, T. D., Washburn, L., Hamilton, M. K., and Mitchell, B. G. 1989, Deep-Sea Res. I, 36, 211-222.
50. Bishop, J. K. B., Davis, R. E., and Sherman, J. T. 2002, Science, 298, 817-820.
51. Boss, E., Pegau, W. S., Gardner, W. D., Zaneveld, J. R. V., Barnard, A. H., Twardowski, M. S., Chang, G. C., and Dickey, T. D. 2001, J. Geophys. Res., 106, 9509-9516.
52. Twardowski, M., Boss, E., MacDonald, J. B., Pegau, W. S., Barnard, A. H., and Zaneveld, J. R. V. 2001, J. Geophys. Res., 106, 14,129-14,142.
53. Boss, E., Pegau, W. S., Lee, M., Twardowski, M., Shybanov, E., Korotaev, G., and Baratange, F. 2003, The particulate backscattering ratio at LEO 15 and its use to study particle composition and distribution, J. Geophys. Res., in press.
54. Coble, P.G., 1996, Mar. Chem., 51, 325-346.
55. Petrenko, A. A., Jones, B. H., Dickey, T. D., LeHaitre, M., and Moore, C. 1997, J. Geophys. Res., 102, 25,061-26,071.
56. O'Reilly, J. E., Maritorena, S., Mitchell, B. G., Siegel, D. A., Carder, K. L., Garver, S. A., Kahru, M., and McClain, C. 1998, J. Geophys. Res., 103, 24,937-24,953.
57. Behrenfeld, M. and Falkowski, P. G. 1997, Limnol. Oceanogr., 42, 1479-1491.
58. Kahru, M. and Mitchell, B. G. 2001, J. Geophys. Res., 106, 2517-2529.
59. Arnone, R. A., Martinolich, P., Gould, R. W., Sydor, M., Stumpf, R., and Ladner, S. 1998, Coastal optical properties using SeaWiFS, Proceedings from Ocean Optics XVI, Kona, HI, CD-ROM.
60. Gould, R. W., Jr., Arnone, R. A., and Martinolich, P. M. 1999, Appl. Opt., 38, 2377-2383.
61. Arnone, R. and Gould, R. W. 2001, Backscatter, 12, 17-24.
62. Gould, R. W., Jr. and Arnone, R. A. 2003, Three-dimensional fields of salinity and total suspended solids derived from ocean color satellite imagery, J. Atmos. Ocean Tech., submitted.
63. Snyder, W. A., Donato, T., Bachmann, C., Bowles, J., Davis, C. O., Fusina, R., Lamela, G., Rhea, W. J., and Lathrop, R. 2002, Depth and bottom type estimates of a turbid shallow water estuary using visible/near IR hyperspectral remote sensing reflectance, Proceedings from Ocean Optics XVI, Santa Fe, NM, CD-ROM.
64. Hill, V., Weeks, A., Darecki, M., and Robinson, I. 2000, Phytoplankton signatures in hyperspectral absorption data, Proceedings from Ocean Optics XV, Monte Carlo, Monaco, CD-ROM.
65. Gower, J. F. R., Doerffer, R., and Borstad, G. A. 1990, Int. J. Rem. Sens., 11, 313-320.
66. Gower, J. F. R., Doerffer, R., and Borstad, G. A. 1999, Int. J. Rem. Sens., 20, 1771-1786.
67. Babin, M., Morel, A., and Gentili, B. 1996, Int. J. Rem. Sens., 17, 2417-2448.
68. Letelier, R. M. and Abbott, M. R 1996, Rem. Sens. Environ., 58, 215-223.
69. Johnsen, G. and Sakshaug, E. 2000, S. Afr. J. Mar. Sci., 22, 309-321.
70. Cullen, J. J., Ciotti, A. M., Davis, R. F., and Lewis, M. R. 1997, Limnol. Oceanogr., 42, 1223-1239.

71. Schofield, O., Grzymski, J., Bissett, W. P., Kirkpatrick, G. J., Millie, D. F., Moline, M., and Roesler, C. S. 1999, J. Phycol., 35, 1477-1496.
72. Stumpf, R. P. 2001, Human and Ecological Risk Assessment, 7, 1363-1368.
73. Weidemann, A. D., Johnson, D. J., Holyer, R. J., Pegau, W. S., Jugan, L. A., and Sandidge, J. C. 2000, Rem. Sens. Environ., 76, 260-267.
74. Chang, G. C. and Dickey, T. D. 1998, The 1998 WHOI/IOS/ONR Internal Solitary Wave Workshop: Contributed Papers, WHOI-99-07, T. Duda (Ed.), Woods Hole Oceanographic Institution, Woods Hole, MA, 65-68.
75. Johnson, D. R., Weidemann, A., and Pegau, W. S. 2001, Cont. Shelf Res., 21, 1473-1484.
76. Bogucki, D., Dickey, T., and Redekopp, L. 1997, J. Phys. Oceanogr., 27, 1181-1196.
77. Trowbridge, J. H. and Nowell, A. R. M. 1994, Cont. Shelf Res., 14, 1057-1061.
78. Chang, G. C., Dickey, T. D., and Williams, A. J., 3rd 2001, J. Geophys. Res., 106, 9517-9531.
79. Hill, P. S., Voulgaris, G., and Trowbridge, J. H. 2001, J. Geophys. Res., 106, 9543-9549.
80. Dickey, T. D., Chang, G. C., Agrawal, Y. C., Williams, A. J., 3rd, and Hill, P. S. 1998, Geophys. Res. Lett., 25, 3533-3536.
81. Agrawal, Y. C. and Traykovski, P. 2001, J. Geophys. Res., 106, 9533-9542.
82. Abbott, M. R. and Letelier, R. M. 1998, Deep-Sea Res. II, 45, 1639-1667.